Applied Catalysis B: Environmental 138–139 (2013) 342–352

Contents lists available at SciVerse ScienceDirect

Applied Catalysis B: Environmental

journal homepage: www.elsevier.com/locate/apcatb

Sulphur tolerance of a P-doped Rh/γ-Al_2O_3 catalyst during the partial oxidation of methane to syngas

S. Cimino [a,*], G. Mancino [b], L. Lisi [a]

[a] Istituto Ricerche sulla Combustione CNR, Napoli, Italy
[b] Dipartimento Ingegneria Chimica Università di Napoli Federico II, Italy

ARTICLE INFO

Article history:
Received 20 December 2012
Received in revised form 11 February 2013
Accepted 18 February 2013
Available online 4 March 2013

Keywords:
Rh
Sulphur poisoning
Catalytic partial oxidation
Structured catalyst
DRIFT

ABSTRACT

A novel monolith catalyst with Rh supported on γ-Al_2O_3 and doped with phosphorous was prepared by temperature-programmed reduction of oxidic precursors and tested for the first time in the CPO of methane at short contact time and high temperature in the presence of sulphur. The catalyst was characterized by ICP-MS, XRD, TGA, SEM-EDS, BET, H_2-TPR, quantitative CO chemisorption measurements and in situ DRIFT of adsorbed CO, performed on freshly reduced samples or after exposures to sulphur species at temperatures and conditions close to those expected under actual CPO of methane. Results were compared with the reference undoped Rh/γ-Al_2O_3 catalyst and the P-γ-Al_2O_3 support. Both transient and steady state operation of the CPO reactor were investigated particularly with regards to the effect that the addition/removal of variable S quantities in the feed has on catalyst temperature, on the formation of main reaction products, on the approach to equilibrium and on the apparent reaction rate.

1. Introduction

The catalytic partial oxidation (CPO) of methane over precious metal catalysts has been shown to be an attractive way to obtain syngas (CO and H_2) in small autothermal reactors at extremely short contact times (10^{-2} to 10^{-4} s) and >90% selectivity to H_2 and CO [1–3]. Rh-based systems are commonly recognized as the best performing catalysts in terms of high activity and selectivity to syngas during the CPO of hydrocarbons from methane up to diesel and jet-fuels [1,3]. Moreover Rh-based catalysts have been proved to gasify autothermally lignocellulosic biomass in millisecond contact times in oxygen deficient conditions, producing a syngas stream free from tars and chars through the reactive flash volatilization technique [4,5]. However rhodium is among the scarcest and most expensive precious metals, having mainly no viable substitute for the reduction of NO_x in three-way automotive catalysts [6,7]. Only recently the possible poisoning effects due to inorganic elements on the costly Rh catalysts have been recognized as a serious drawback of CPO and related technology [8–11]. In particular the presence of even small amounts of sulphur in the feed to a methane CPO reactor has a marked negative impact on fuel conversion and H_2 selectivity [10–13]. Poisoning is due to the adsorption of S directly onto Rh active sites, mainly causing a (reversible) suppression of their steam reforming activity [10,12,13], with an associated risk of catalyst overheating during CPO autothermal operation [14]. Pt-based catalysts are less active for steam reforming reactions but in turn are more S-tolerant [8,12,15]. A qualitative similar inhibiting effect has been found for the CPO of ethane on Rh/γ-Al_2O_3 [16], even if the adverse impact of S becomes progressively smaller with more reactive hydrocarbon feeds [9]. Therefore it is desirable to develop catalysts intrinsically sulphur tolerant and not readily poisoned by the amounts of sulphur commonly found in fuels such as natural gas (typically 8-10ppmv added in pipeline gas) or left in heavier fuels or biomass derived feedstocks even after a preliminary desulphurization.

In fact studying the effect of several inorganics on methane steam reforming activity of Rh/α-Al_2O_3 catalysts poisoned ex situ, Schmidt and co-workers [17] reported that sulphur decreased the methane conversion the most, followed by phosphorus, potassium and sodium whereas, calcium, magnesium and silicon caused negligible changes in methane conversion. Although phosphorous is recognized as a common poison for metal catalysts [17,18], a substantial body of literature has shown that metal phosphide catalysts (particularly those based on MoP and Ni_2P) have promising hydrodesulphurization (HDS) properties [19–26]. Recently, some reports on novel supported noble metal phosphides for deep HDS process [27,28] have shown that Rh_2P/SiO_2 catalysts display superior activity, and sulphur tolerance than the corresponding supported Rh catalyst (either sulphided or not) and a commercial Ni-Mo/Al_2O_3 catalyst. Bulk and SiO_2 supported Rh_2P catalysts have been readily obtained by temperature programmed reduction of

* Corresponding author at: Istituto Ricerche sulla Combustione – CNR – P.le V. Tecchio 80, 80125 Napoli, Italy. Tel.: +39 081 7682233.
E-mail addresses: stefano.cimino@cnr.it, stcimino@unina.it (S. Cimino).

0926-3373/$ – see front matter © 2013 Elsevier B.V. All rights reserved.
http://dx.doi.org/10.1016/j.apcatb.2013.02.039

oxide precursors [27–29]: while Rh_2P preserves a metallic nature and is stable at high temperature, its catalytic properties are different from those of Rh metal (and Rh sulphides). The enhanced resistance to S-poisoning seems directly related to the presence of P in the Rh_2P particles, which inhibits the irreversible adsorption of S at the particle surface as well as the incorporation of S into the bulk (i.e. to form Rh sulphide) [27]: XPS analysis of a HDS-tested 5 wt.% Rh_2P/SiO_2 catalyst showed no evidence for surface sulfur, and sulphidation with a 3% H_2S/H_2 mix at 300 °C yielded a S/Rh ratio which was over four times lower than for the reference Rh/SiO_2 catalyst.

At the same time the surface P does not appear to suppress CO adsorption on Rh, preserving it even in the presence of S, which is the reason for the high catalytic activity [27,28]. However some contrasting evidence for the catalytic properties of P-enriched Rh/Al_2O_3 come from an older study by Muetterties and Sauer [30] who found a substantial reduction in the hydrogenation activity for either sulphided or phosphided (with PH_3 at 300 °C) catalysts with respect to the reference Rh/Al_2O_3.

This points to the importance of the preparation route employed to achieve an effective interaction between P and Rh as well as to the role and the nature of the support. In fact alumina is generally recognized as an effective support for Rh in partial oxidation and steam reforming catalysts: it ensures a good metal dispersion and sintering resistance, it may participate to reaction via reverse spill-over of adsorbed hydroxyl species [31], and it generally ensures a better sulphur tolerance than other refractory oxides [32,33]. Recently, amorphous aluminium phosphate ($AlPO_4$) has been identified as a more efficient support material to produce optimum metal-support interactions that can reduce significantly Rh loading in automotive three way catalysts, owing to thermally stable and highly dispersed Rh nanoparticles anchored strongly onto the phosphate surface via the formation of Rh—O—P bondings [7,34].

With such premises in mind, in this work we set out to investigate the possible beneficial effect of P-doping of Rh supported on La-γ-Al_2O_3 with regards to catalytic activity and S-tolerance during the self-sustained methane CPO at short contact time. Phosphorous was co-impregnated with Rh on the support and the catalyst was pre-reduced in H_2 at 900 °C in order to maximize the possible interactions between components and to stabilize the active phase at the high temperatures typically encountered in the CPO process.

The novel P-doped Rh catalyst, prepared in powder form or washcoated onto cordierite honeycombs, was characterized by ICP-MS, XRD, TGA, SEM-EDS, BET, H_2-TPR, quantitative CO chemisorption measurements and in situ DRIFT of adsorbed CO, performed on fresh samples or after exposures to sulphur species at temperatures and conditions close to those expected under actual CPO of methane. Results were compared with the reference undoped $Rh/La\text{-}\gamma Al_2O_3$ catalyst and the P-alumina support. Both transient and steady state operation of the CPO reactor were investigated particularly with regards to the effect that the addition/removal of variable S quantities in the feed has on catalyst temperature, on the formation of main reaction products, and on the approach to equilibrium.

2. Experimental

2.1. Catalyst preparation

Rh catalyst doped with phosphorous and supported on a 3% w/w La_2O_3-stabilised γ-Al_2O_3 (SCFa140-L3 Sasol) was prepared via a incipient wetness co-impregnation procedure using an aqueous acid solution of $Rh(NO_3)_3$ and $(NH_4)H_2PO_4$ (Aldrich). Precursors were dosed at a P/Rh atomic ratio of 0.7 in order to obtain a target loading of 1.0% w/w of Rh in the catalyst through 2 impregnation cycles. Following drying in stove at 120 °C and calcination in air at 550 °C for 2 h after each impregnation step, the catalyst was finally reduced in a 2% H_2/Ar mix by heating at 10 °C/min between room temperature and 900 °C, and holding for 1 h at this temperature. The excess of P with respect to the formation of Rh_2P (P/Rh = 0.5) was selected in order to maximize phosphide formation during TPR as suggested in [27]. Two reference powder samples were also prepared with the same nominal content of Rh or P by excluding either phosphorous or rhodium precursors from the impregnating solution while keeping all the rest the same. According to their elemental composition, samples were labelled as Rh-P/LA, Rh/LA and P/LA, where LA represents the lanthanum stabilized γ-Al_2O_3. When desired, the reduced catalysts were subjected to controlled sulphurization in a fixed bed quartz reactor at 800 °C for 1 h under a flow of H_2S/H_2 (20 ppm/1.8%, balance N_2) at atmospheric pressure, and then exposed to air at room temperature.

Monolith samples were prepared applying the same procedure to honeycomb samples previously washcoated with the LA support. In particular commercial honeycomb monoliths with straight and parallel channels of roughly square section (cordierite, 600 cpsi by NGK) were cut in the shape of disks of ca. 17 mm diameter and 10 mm length and washcoated by a modified dip-coating procedure [35]. The final loading of active phase (Rh-P/LA) applied on the honeycombs was 0.11 g/cm^3, corresponding to a nominal average thickness of the washcoat of ca. 20 μm.

2.2. Catalyst characterization

Elemental content was quantitatively determined on selected fresh and used catalysts by inductively coupled plasma spectrometry (ICP) on an Agilent 7500 ICP-MS instrument, after microwave-assisted digestion of samples in nitric/hydrochloric acid solution.

Thermogravimetric analysis of uncalcined powder samples were run in PerkinElmer Pyris 1TGA by ramping up to 900 °C at 10 °C/min in flowing air or 2% H_2/N_2 mixture. Gaseous products, sampled via a heated transfer line, were analyzed with a FTIR spectrometer (PerkinElmer Spectrum GX).

XRD analysis was performed on powder samples with a Bruker D2 Phaser diffractometer (operated at diffraction angles ranging between 10 and 80° 2θ with a scan velocity equal to 0.02° 2θ s^{-1}).

Scanning electron microscopy (SEM) was carried out on honeycomb catalysts with a FEI Inspect microscope equipped with an energy dispersive X-ray (EDX) probe.

BET specific surface area measurements were performed with a Quantachrome Autosorb 1-C by N_2 adsorption at 77 K after degassing samples for 2 h at 150 °C; in the case of honeycomb catalysts the surface area was assigned only to the active washcoat layer (SA of cordierite substrate $\leq$ 1 m^2/g).

Temperature programmed reduction (TPR) experiments were carried out with a Micrometrics AutoChem 2020 equipped with a TC detector on catalysts and supports pre-treated in air at 550 °C. The sample powder (200–400 mg) was heated at 10 °C/min between room temperature and 900 °C in flowing 2% H_2/Ar mix (50 cm^3/min).

CO chemisorption measurements were also performed in the same Quantachrome Autosorb 1-C instrument. Rh catalysts and their corresponding alumina supports (ca. 200 mg) were pretreated at 400 °C under a flow of pure H_2 for 1 h, then evacuated for 2 h at the same temperature and cooled under vacuum to 40 °C, where CO adsorption was performed using the method of the double isotherm [36] with an intermediary treatment under vacuum (P = 0.001 mm Hg). The first isotherm gives the total amount of chemisorbed CO, the second isotherm gives the reversible part of chemisorbed CO, the difference between the two isotherms giving the irreversible part of chemisorbed CO. The two isothermal curves were drawn with 5–10 experimental points in the 20–800 mm Hg

pressure domain. The total and reversible adsorption curves do not always exhibit a saturation plateau; the monolayer CO chemisorption was obtained from the extrapolation at zero pressure of the linear part of the irreversible strong adsorption [36]. Since CO may adsorb on Rh in several forms (linear, bridged, di-carbonyl species) [36–39] mainly depending on metal dispersion, type of support and catalyst pre-treatment, the adsorption stoichiometry (CO/M) is not known a priori, and it was assigned by the corresponding DRIFT study.

DRIFT experiments were performed in a PerkinElmer Spectrum GX spectrometer equipped with a liquid-N_2 cooled MCT detector with a spectral resolution of 4 cm^{-1} and averaged over 50 scans. For each experiment approximately 30 mg of finely ground powder sample was placed into the ceramic cup of a commercial high-temperature Pike DRIFT cell equipped with a ZnSe window and connected to mass flow controlled gas lines. The sample was then treated in the following way: (i) prior to the experiments the sample was reduced in pure H_2 for 1 h at 400 °C, purged with Ar (100 cm^3/min) for about 1 h and then cooled down to 40 °C under the same flow before a background spectrum was recorded; (ii) CO was adsorbed at this temperature by flowing a 5% CO/N_2 mixture (100 cm^3/min) for 1 h. IR spectra were recorded both under CO flow and during prolonged flushing with Ar (100 cm^3/min). All spectra were ratioed against the corresponding background spectra collected on the adsorbate-free sample at 40 °C. Sulphurization of catalysts was performed in the same cell: the sample was heated up to 800 °C under a 2% H_2/N_2 flow, followed by exposure to $H_2S/H_2/N_2$ mixture (20 ppm/1.8%/rest, 200 cm^3/min) for 1 h, and then purged and cooled down under Ar flow, before CO adsorption. The effect of regeneration of sulphurized catalysts by reduction at 400 °C under a H_2 flow for 1 h (and purging at the same temperature) was also investigated.

2.3. Catalyst testing

P-doped Rh/La-Al_2O_3 honeycomb catalysts were tested for the CPO of methane to syn-gas in a lab scale reactor operated at nearly atmospheric pressure under self-sustained short contact time conditions using (simulated) air as oxidant. The catalytic honeycomb was stacked between two mullite foam monoliths (45 ppi, L = 12 mm) as heat shields and placed in a quartz tube inserted in an electric furnace that was used for pre-heating (fixed at 235 °C). High-purity gases (CH_4, O_2, N_2, SO_2 208 ppm in N_2) calibrated via Brooks 5850-MFCs, were pre-mixed and fed to the reactor at a total flow 135 Sl/h, corresponding to a gas hourly space velocity GHSV = 8×10^4 h^{-1} (based on the empty volume of the honeycomb). The impact of sulphur addition (2–58 ppmv SO_2) was investigated at fixed CH_4/O_2 feed ratio = 2 (stoichiometric for syngas production), under both transient and steady state conditions, by partially substituting the N_2 flow in the feed with an equal flow of the SO_2 in N_2 mix. Reactor temperatures were measured by means of K-type thermocouples (d = 0.5 mm) placed in the middle and at the exit of the central channel of the catalytic honeycomb (T_{cat} and T_{out}), as well as in the gas downstream of heat shield. Further details on the lab scale experimental set up were already reported elsewhere [13,15].

Hot product gases passed through a condenser and a $CaCl_2$ trap to remove water, and a continuous analyzer (syngasGEIT) was employed to measure the concentrations of CO, CO_2 and CH_4 (ND-IR), O_2 (ECD), and H_2 (TCD, with cross sensitivity corrections). O_2 was always completely converted under steady state operation as well as during transient addition/removal of S to the feed. H_2O production was calculated from the O-balance. Carbon and hydrogen balances were closed within ±1% and ±2%, respectively. Methane conversion, yields and selectivities to CO and H_2 were calculated according to the following definitions based on measured dry mol fractions:

$$x_{CH_4} = 100\left(1 - \frac{CH_4^{out}}{CH_4^{out} + CO_2^{out} + CO^{out}}\right);$$

$$Y_{CO} = 100\left(\frac{CO^{out}}{CH_4^{out} + CO_2^{out} + CO^{out}}\right);$$

$$S_{CO} = 100\left(\frac{Y_{CO}}{x_{CH_4}}\right)$$

$$Y_{H_2} = \frac{100}{2}\left(\frac{H_2^{out}}{CH_4^{out} + CO_2^{out} + CO^{out}}\right);$$

$$S_{H_2} = 100 \times 2\left(\frac{Y_{H_2}}{x_{CH_4}}\right)$$

The fate of sulphur was determined by gas chromatography employing a high sensitivity dual plasma sulphur chemiluminescence detector (SCD, Agilent) and a GasPro column. It was confirmed that under the typical CPO operating conditions, i.e. high H_2 partial pressure and high temperatures (>700 °C), all of the sulphur is transformed into H_2S (with traces of COS), in agreement with thermodynamic predictions.

Equilibrium calculations with constant enthalpy and pressure were performed using CHEMKIN 4.1.1 software excluding solid carbon formation, which was never observed experimentally.

3. Results and discussion

3.1. Catalyst characterization

Table 1 illustrates catalysts denomination and final pre-treatment, loading of active phase in honeycombs, elemental composition and BET specific surface area.

Preliminary thermogravimetric analysis of the mono basic ammonium phosphate precursor (supplementary data) confirmed that its decomposition in air proceeded in 2 main steps: roughly 30% of the initial weight was lost in the temperature range from 130 °C to ca. 400 °C corresponding to the evolution of ammonia and water; the remaining phosphorous oxide was quickly and completely devolatilized above 430 °C [41]. A similar behaviour was observed when heating in H_2/N_2 flow, with an increase in this critical temperature by 50–60 °C. In contrast, TGA profiles of the LA alumina support impregnated with the same phosphorous precursor, indicated that no significant loss of phosphorous occurred when heating up to 900 °C (in air or H_2/N_2) due to the strong interaction with alumina and possible formation of superficial amorphous aluminium or lanthanum phosphates [20], which, however were not detected by XRD analysis.

Accordingly, the amount of elemental phosphorous found by ICP-MS in the catalysts after the final TPR treatment at 900 °C (Table 1) was in line with its nominal content (0.2%); Rh and La were also detected at levels close to their nominal ones.

Values of the BET specific surface area are reported in Table 1: phosphorous addition to the commercial La-γ-Al_2O_3 (LA) and subsequent reducing treatment at 900 °C did not alter the initial surface area of the support (140 m^2/g). The presence of rhodium determined a limited decrease in this value down to 131 m^2/g for the reduced Rh-P/LA sample, and 122 m^2/g for the reference Rh/LA sample, thus suggesting a positive stabilizing effect obtained via doping with phosphorous. The active layer in honeycomb Rh-P/LA catalysts displayed a value of 123 m^2/g, only slightly lower than

Table 1
Denomination of catalysts and supports, final pre-treatment, honeycomb loading, elemental composition and BET surface area.

	Pretreatment	Loading (g/cm^3)[a]	Rh (w/w %)[b]	P (w/w %)	La (w/w %)	BET (m^2/g)[b]
LA	As received		–	–	2.6	143.0
P/LA	TPR 900 °C		–	0.30	2.6	139.8
Rh-P/LA	TPR 900 °C		0.98	0.19	2.7	130.6
Rh/LA	TPR 900 °C		0.89	–	2.6	122.2
Honeycombs						
Rh-P/LA	TPR 900 °C	0.11	0.99	0.20		122.6
	TPR 1000 °C	0.11				114.7
	Aged in CPO	0.11				112.5

[a] Weight of active washcoat per unit volume of honeycomb catalyst.
[b] With respect to the weight of active catalyst (cordierite substrate excluded).

the reference powder catalyst, possibly due to a small contribution coming from the pseudo-bohemite binder used in the washcoating step [35]. A thermal treatment for 1 h at 1000 °C under reducing atmosphere, as well as the exposure to CPO operation for a total of 38 h, both determined a further limited decrease in the surface area of Rh-P/LA honeycomb catalyst down to 112–115 m^2/g.

SEM observation of longitudinal sections of the honeycomb catalyst (after reduction at 900 °C) revealed that all channels were coated with a rough porous layer consisting of interconnected aggregates of submicronic γ-Al_2O_3 particles which were firmly anchored to the underlying cordierite walls. The average thickness of the washcoat layer was in line with its nominal value (ca 20 μm, estimated by assuming an uniform deposition on the wet geometrical area of honeycomb channels). EDX mapping of elemental distributions (supplementary data) confirmed the simultaneous occurrence and uniform concentration of Rh and P throughout the Al washcoat layer, and not within the macroporous cordierite walls.

Temperature programmed reduction profiles of Rh-P/LA, Rh/LA, and P/LA samples pre-calcined in air at 550 °C are compared in Fig. 1; the corresponding amounts of hydrogen taken up and referred to the actual Rh content are reported in Table 2. The reference P-LA support showed an almost flat baseline up to 870 °C; above this temperature it started to develop a hardly detectable peak, which, in line with previous reports, could be assigned to the reduction of surface aluminium phosphate [21]. H_2 consumption on Rh-LA and Rh-P/LA catalysts started at ca. 65 °C and showed peak maxima respectively at 195 °C and 237 °C with shoulders at 125 °C and 275 °C. Such complex pattern is typical of the reduction of Rh_2O_3 clusters not strongly interacting with the alumina support to metallic Rh [32]. The left shift of the peak temperature observed for the P-doped catalyst is likely related to a higher superficial dispersion of the Rh oxide particles, possibly due to the co-impregnation procedure employing Rh^{+3} and $H_2PO_4^-$ precursors.

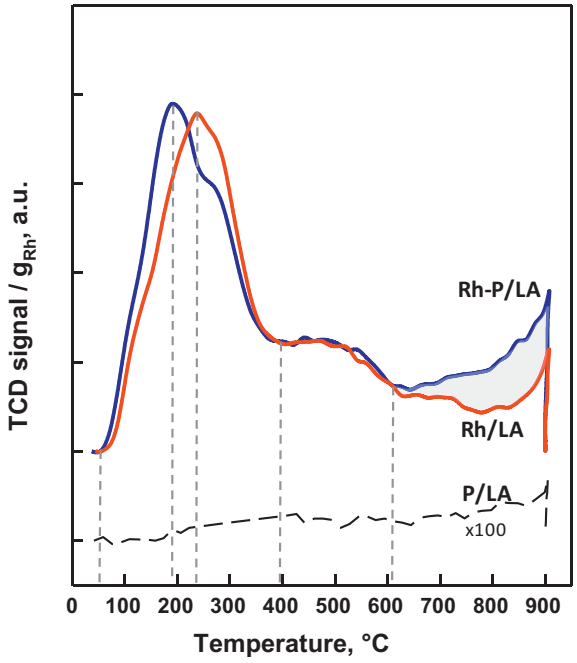

Fig. 1. H_2-TPR profiles for the Rh-P/LA, Rh/LA catalysts and P-LA support calcined at 550 °C in air. For comparison purpose the signal was referred to the actual weight of Rh in catalysts (ca. 1 w/w %), and multiplied × 100 for the support.

A broad and small reduction peak (in the range 350–600 °C) centred at ca. 485 °C appeared in the TPR traces of both Rh catalysts which can be assigned to the reduction of RhO_x species interacting more strongly with the alumina [31,41]. The hydrogen consumption calculated from TPR profiles of Rh/LA and Rh-P/LA catalysts up to ca. 600 °C and referred to the measured content of Rh in each sample (Table 2) corresponded to the complete reduction of Rh^{3+} to Rh^0 for both samples.

A further significant reduction event occurred only for the Rh-P/LA sample starting at temperatures around 600 °C, which was completed under the isothermal step at 900 °C (highlighted area in Fig. 1). That peak, which was absent in the TPR of reference Rh/LA sample, can be assigned to the reduction of phosphate species. Recalling that the reduction of superficial $AlPO_4$ was reported to occur above 830 °C [21] and in our reference P-LA sample it only started above 870 °C, the easier reducibility of phosphates in the Rh-P/LA catalyst was probably due a spill-over effect on Rh sites, which appear to be close enough to interact with phosphorous emerging from the support and to form Rh phosphide species [21]. Assuming that the surplus H_2 consumption (with respect to the full reduction of Rh) was employed to reduce P^{5+} to P^0, then roughly 60% of the initial phosphorous was reduced to the zero oxidation state at the end of TPR. This value can be regarded as an upper limit since the reference Rh-LA sample also showed some H_2 consumption for $T > 850$ °C, which could be related to the surface reduction of aluminium oxide, enhanced by the presence of Rh via a spill-over effect. Therefore, due to the high stability of the superficial $AlPO_4$ species, not all of the phosphorous was available to form a stoichiometric Rh_2P phase even after H_2 reduction at 900 °C: the possible formation of sub-stoichiometric Rh phosphides, or, more

Table 2
H_2-TPR analysis up to 900 °C of the Rh-P/LA and Rh/LA samples.

Sample	T max	H_2^{uptake}/Rh[a]		P/Rh[a,b]	H_2^{uptake}/P[a,d]
		up to 600 °C	Total[c]		
Rh-P/LA	195 °C	1.50	2.44	0.64	1.47
Rh/LA	237 °C	1.49	1.73	–	–

[a] Molar ratio.
[b] By ICP-MS after TPR at 900 °C.
[c] After 1 h at 900 °C.
[d] From H_2 uptake at $T > 600$ °C.

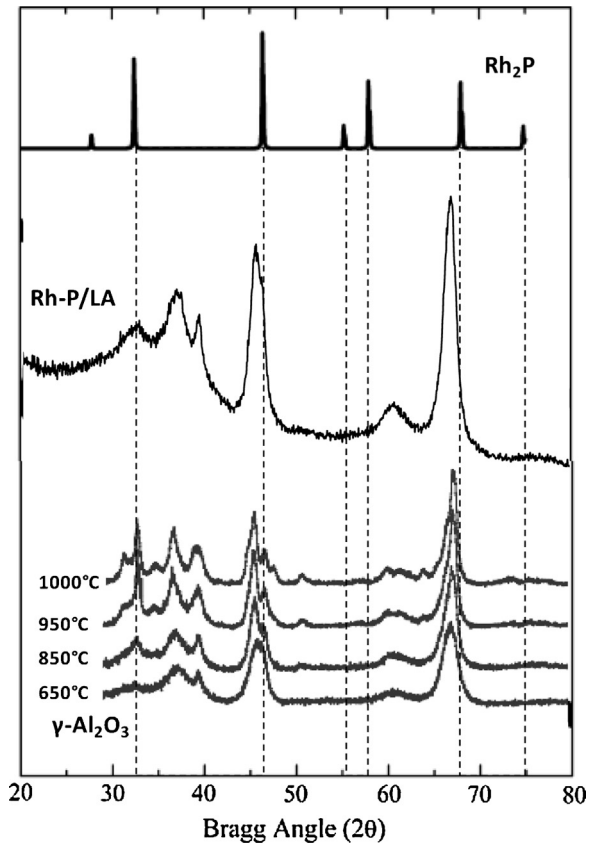

Fig. 2. XRD pattern of Rh-P/LA catalyst after TPR at 900 °C as well as reference patterns for Rh_2P [25] and γ-alumina calcined in air at 650 °C, 850 °C, 950 °C and 1000 °C showing progressive formation of transition δ and θ phases [42].

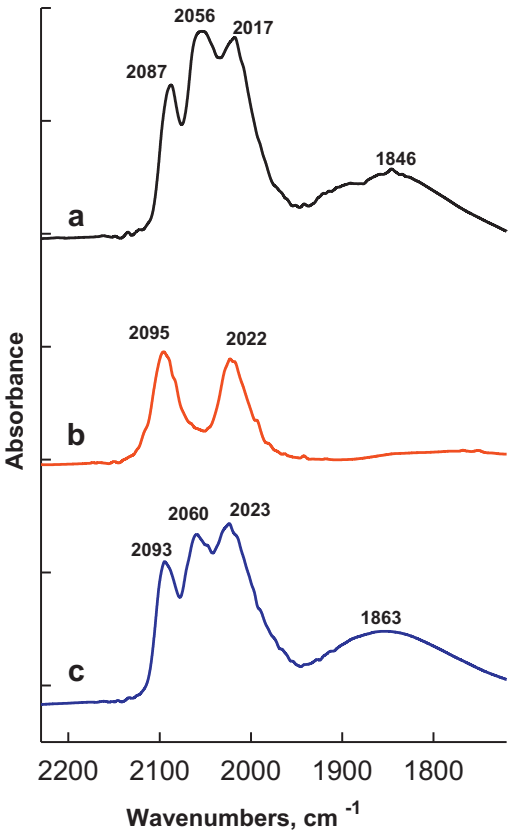

Fig. 3. DRIFT spectra of CO adsorbed over Rh/LA catalyst after 60 min of purging with Ar: (a) freshly reduced sample; (b) following sulphurization at 800 °C in H_2S/H_2; (c) following regeneration at 400 °C in H_2.

simply, the simultaneous presence of both Rh and Rh_2P entities on the surface of Rh-P/LA catalyst cannot be ruled out at the moment.

XRD analysis after the TPR treatment at 900 °C (Fig. 2) failed to identify the formation of Rh_2P species in the Rh-P/LA catalyst, which showed the typical reflections of γ-alumina with incipient formation of transitional δ and θ phases [43]. That is most probably associated to the low loading of active phase, and its high dispersion and possibly its amorphous nature.

Interestingly, TPR profiles of honeycomb supported Rh-P/LA catalysts (not shown) were characterized by features identical to those of the reference powder sample, ruling out any additional effect due to the interaction with the cordierite substrate.

DRIFT and volumetric study of adsorbed CO

After CO adsorption at 40 °C (1 h P_{CO} = 38 mmHg) on freshly reduced catalysts, DRIFT spectra were collected at fixed time intervals under a flow of Ar in order to investigate the nature of surface species and to evaluate the strength of the CO/surface interaction. A common trend was obtained for Rh/LA and Rh-P/LA (respectively, Figs. 3a and 4a), which can be described as follows.

Upon switching to Ar flow, a characteristic band of gaseous CO centred at ca. 2180 cm^{-1} rapidly disappeared and the resulting spectra (exemplified by those recorded after 1 h of Ar purging) were characterized by IR bands in the ranges 2055–2065 cm^{-1} and 1840–1870 cm^{-1}, respectively, attributed to linear and bridged CO adsorbed on large metal particles [37–40]. Such large Rh clusters are not subjected to the disruption of Rh-Rh bond which only takes place when the adsorbed CO is in close proximity of support hydroxyl groups, that is when rhodium species are small and highly dispersed [44–46]. In that case $Rh^{I}(CO)_2$ gem-dicarbonyl species are formed characterized by symmetric and asymmetric stretching bands at around 2090 and 2020 cm^{-1} [37–40,44–46], which indeed were detected for both freshly reduced catalysts (Fig. 3a and Fig. 4a). P doping of Rh particles entailed a significant reduction in the relative intensity of the signal due to linear Rh^0CO species, which was compensated by the simultaneous increase in the bands of gem-dicarbonyl species, whereas the intensity of the broad band due to bridged bond CO was roughly unaltered. The wavenumber values of the gem-dicarbonyl stretching bands were not affected by P-doping, whereas the νCO for linear and bridge bonded CO shifted to higher frequencies, likely due to the transfer of electron density from Rh to P, as also observed for alumina supported nickel-phosphorous catalysts [25,47].

IR bands of bridge- and linear-bonded carbonyls coordinated over metallic Rh particles progressively disappeared (in that order) during prolonged purging in Ar, possibly because of the weak nature of their σ-bond [40,48] making those species relatively less stable [49]. On the other hand gem-dicarbonyl species are quite stable as a result of a strong covalent σ-bond and π-back bond [40,49], and indeed their characteristic IR bands persisted even after prolonged purging.

Regarding sulphurized catalysts, H_2S chemisorption on Rh is reported to be mainly dissociative [50–52] with H_2 evolution; adsorbed S atoms are preferentially bonded to defect sites such as steps [52]. For this reason smaller Rh particles, with their lower surface coordination number and higher density of defect sites are more seriously affected by S poisoning [13,18,53], which in turn is highly selective at low coverages.

DRIFT spectra of CO adsorbed over the catalysts previously sulphurized at 800 °C (and purged in Ar at the same temperature) are reported in Figs. 3b and 4b, and show a general decrease in

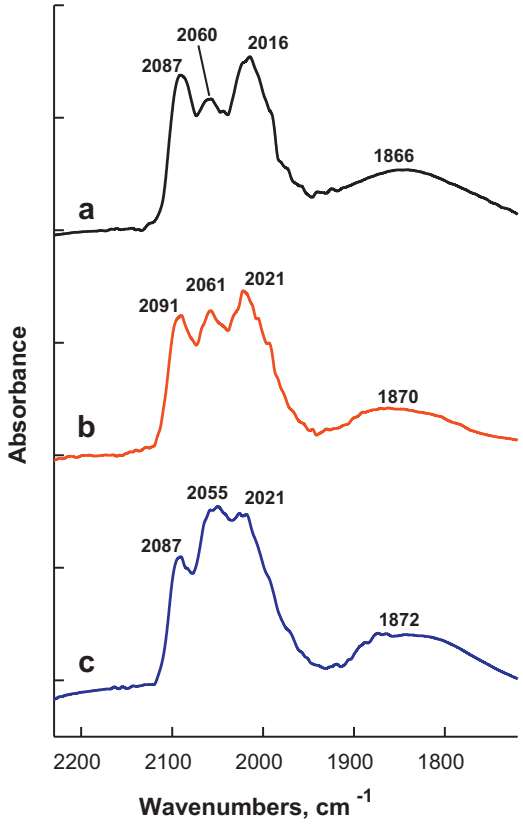

Fig. 4. DRIFT spectra of CO adsorbed over Rh-P/LA catalyst after 60 min of purging with Ar: (a) freshly reduced sample; (b) following sulphurization at 800 °C in H_2S/H_2; (c) following regeneration at 400 °C in H_2.

the intensities of the relevant bands due to an overall lowering of chemisorption capacity (see later). Sulphur had a much stronger impact on the reference Rh/LA catalyst since IR bands corresponding to linear and bridge-bonded CO species disappeared completely (Fig. 3b). The non occurrence of bridge-bonded CO is easily rationalized by the conventional site blocking model; even at low sulphur coverages, the remaining surface Rh atoms become isolated from each other [54]. However, the lack of linear CO species suggests a high degree of sulphur coverage with extensive formation of surface Rh sulphides.

The only mode of CO adsorption over Rh/LA after sulphurization was related to formation of gem-dicarbonyl species, whose characteristic doublet bands were detected at 2022 cm^{-1} and 2095 cm^{-1} and were retained even after prolonged purging with Ar. The wavenumber values were clearly shifted to higher frequencies with respect to the freshly reduced catalyst, which could be explained by withdrawing of the electron density from the metal particles induced by adsorbed sulphur [18,25,47,55]. In conclusion, the electronegative sulphur atoms might leave adjacent Rh atoms with a net positive charge thus facilitating the adsorption of 2 CO molecules [54]. In that case, the occurrence of gem-dicarbonyl species in the sulphurized sample would not be necessarily (or cannot be directly) associated to the morphology and size of supported Rh particles [40 and ref. therein].

Following regeneration in H_2 at 400 °C, the IR bands of linear and bridge bonded CO re-appeared over the sulphurized Rh/LA catalyst (Fig. 3c): as for the freshly reduced sample those species showed a relatively weak bond and progressively disappeared during purging. On the contrary, the intensities of bands for gem-dicarbonyl CO species were not affected significantly by this regeneration and persisted during purging. Due to the high stability of adsorbed S species, their desorption as H_2S is unlikely under those regeneration conditions [52]. However it is conceivable that the reformation of linear- and bridge-bonded CO was related to surface reconstruction and/or partial hydrogenation at 400 °C causing the exposure of some additional Rh sites capable of weakly adsorbing CO [54]. It should be noted that the disappearance of the linear CO adsorption mode on sulphurized Rh/alumina catalyst was not found in previous literature reports likely because the catalysts were pre-treated in H_2 prior to readsorbing CO [54].

Fig. 4b shows the addition of phosphorous in Rh-P/LA catalyst limited the impact of the sulphurization treatment on CO adsorption. In contrast to what observed for the unpromoted catalyst, the IR spectra revealed the simultaneous presence of all the three modes of CO adsorption, while confirming a higher stability of geminal species upon prolonged purging. In particular, the intensity of the band at 2061 cm^{-1} assigned to linear CO species became comparable to those doublet bands of geminal carbonyls respectively at 2091 cm^{-1} and 2021 cm^{-1}; at the same time, bridged CO species showed a broad band with a lowered relative intensity and a maximum shifted to 1870 cm^{-1}. Therefore sulphurization determined an upward shift of all the characteristics wavenumbers of CO adsorption modes: however, this was less pronounced when Rh was promoted with P, possibly suggesting a lower weakening of the metal—CO bond induced by adsorbed S [25,56]. As for the unpromoted Rh/LA catalyst, regeneration in H_2 at 400 °C of Rh-P/LA sulphurized sample caused some partial surface reconstruction/hydrogenation, which in turn increased only the intensity of the bands for bridge- and linear-bonded CO (Fig. 4c).

The quantitative results of CO chemisorption measurements performed at 40 °C on reduced samples and following sulphurization at 800 °C (+H_2 regeneration at 400 °C) are summarized in Table 3 (total, weak and irreversible CO adsorption isotherms for each catalyst and support are reported in the supplementary material). P-LA and LA supports had identical adsorption isotherms, which only accounted for a reversible CO physisorption, thus excluding any direct contribution of phosphorous; furthermore CO adsorption on the supports was not altered by the sulphurization treatment.

Comparing results obtained on freshly reduced catalysts confirms the addition of surface phosphorous did not suppress CO adsorption on Rh but in fact it caused a significant increase in the amount of irreversibly chemisorbed CO, which was ca. 60% higher for the Rh-P/LA sample than for the undoped Rh/LA (Table 3 first column). Moreover the weak isotherm recorded over the catalysts containing Rh was higher than the curve corresponding to the physisorption of CO on the support. Thus some additional CO was absorbed on the noble metal and bonded to its surface weakly, since it didn't resist to sample evacuation: the corresponding CO amounts were estimated by extrapolating to zero pressure the difference between the two reversible adsorption curves and were similar for the two catalysts (CO weak ads., Table 3).

In agreement with previous reports [37,40,44], our DRIFT experiments of CO adsorption on P-doped and undoped Rh catalysts showed the simultaneous presence of prevailing gem-dicarbonyl species, together with some linear bonded and bridged CO species on larger Rh clusters. However, those last two species disappeared progressively when purging the sample with Ar. Based on those results, CO/Rh stoichiometric coefficients were assumed equal to 2 and 1 respectively for the strong and weak adsorption components on Rh, allowing to distinguish the contribution of isolated Rh sites (SAs) and larger metal clusters (SAw) to the total exposed surface area (Table 3). The contribution from bridge bonded CO species to the weak adsorption was neglected according to previous literature data on Rh/alumina reporting high values of the linear to bridging adsorbed CO ratio (above 20 [40]).

Table 3
Results of CO chemisorption measurement at 40 °C on freshly reduced and sulphurized samples: strong and weak chemisorbed CO (at zero pressure), corresponding values of exposed metal surface areas (SAs, SAw), percentage metal dispersion and average diameter of crystallites (d).

Sample pretreatment	CO strong ads. (μmol/g_{cat})	CO weak ads. (μmol/g_{cat})	SA[a] s (m^2/g_{cat})	SA[b] w (m^2/g_{cat})	SA s + w (m^2/g_{cat})	dispersion (%)	*d* (nm)
TPR 900 °C + H_2 400 °C							
Rh-P/LA	80.4	8.7	1.82	0.39	2.21	51.3	2.14
Rh/LA	49.5	7.6	1.12	0.34	1.46	37.5	2.93
P/LA	0	0	–	–	–	–	–
H_2S/H_2 800 °C + H_2 400 °C							
Rh-P/LA	34.8	17.8	0.79	0.81	1.60	37.0	
Rh/LA	14.3	13.7	0.32	0.61	0.93	23.8	
P/LA	0	0	–	–	–	–	–
LA	0	0	–	–	–	–	–
H_2S/H_2 800 °C + H_2 800 °C							
Rh-P/LA	43.3	12.9	0.98	0.59	1.57	36.3	
Rh/LA	35.7		0.81				
LA	5	0	–	–	–	–	–

[a] CO/Rh = 2.
[b] CO/Rh = 1.

The addition of phosphorous effectively increased metal dispersion up to 51.3% corresponding to an average diameter of the metal particles down to 2.1 nm, as opposed to 37.5% dispersion and 2.9 nm calculated for the reference undoped Rh catalyst. Apart from the smaller dimensions of the precursor Rh_2O_3 crystallites on the P-doped alumina inferred by TPR analysis, the formation of a Rh-P metallic phase with the phosphorous released from the support might effectively contribute to re-disperse Rh clusters [21]. Furthermore, it was reported that sintering of Rh nanoparticles on phospated alumina is inhibited due to a strong metal-support interaction [7,34].

Table 3 presents values of strongly and weakly adsorbed CO and exposed metal surface area after sulphurization for 1 h at 800 °C with the H_2S/H_2 mix, and following a new pre-treatment at 400 °C for 1 h in H_2. It should be noted that samples tested under those conditions can be considered as regenerated catalysts. Indeed, the H_2 pre-treatment at 400 °C was necessary due to the exposure to air after sulphurization carried out ex situ. The strong sulphur adsorption occurring on Rh sites caused a reduction in the total CO adsorption capacity, which was also accompanied by an increase in the amount of weakly bonded CO. As a consequence the difference between the two isotherms was significantly lower, but still independent of the pressure level and precise enough to calculate the irreversible fraction adsorbed CO (Table 3). Due to the presence of phosphorous, the Rh-P/LA catalyst preserved an irreversible chemisorption capacity which was more than two times larger than on the reference Rh/LA system. This agrees well with previous results [27] showing that following a H_2S/H_2 treatment at 300 °C the site blockage by S on a Rh_2P/SiO_2 catalyst was roughly halved with respect to its reference Rh/SiO_2. Following sulphurization, both catalysts adsorbed weakly on their metal particles almost twice as much CO as their freshly reduced counterparts (Table 3).

The strong decrease in the amount of irreversibly adsorbed CO suggests that highly dispersed Rh sites, are preferred targets for S adsorption [15,18,53], whilst larger metal clusters appear less affected. The simultaneous increase in the amount of weakly bonded CO confirms the qualitative trend observed during DRIFT experiments and was related to the partial surface reconstruction/hydrogenation occurring on the sulphurized sample during the H_2 treatment at 400 °C.

Assuming unaltered stoichiometric coefficients, the residual metal surface areas available for CO adsorption on Rh-P/LA and Rh/LA catalysts were lowered respectively to 72% and 63% of their initial values. However, if we limit to the impact of sulphur on those metal sites capable to strongly adsorb CO, the values of SAs for Rh-P/LA and Rh/LA dropped to respectively 42% and 24% of their initial levels. It clearly comes out that P-addition helped to preserve a much higher active surface area (0.79 m^2/g vs. 0.32 m^2/g) of those isolated and coordinatively unsaturated Rh surface atoms which are generally reported to decrease the energy required to form relevant transition states for the initial C—H bond activation step in reforming reactions [57]. Increasing further the temperature of the H_2 pre-treatment up to 800 °C, the sulphurized Rh-P/LA catalyst recovered some but not all of its strong CO chemisorption capacity (Table 3), suggesting that complete regeneration is a rather slow process and/or some catalyst reconstruction had occurred. However a precise evaluation of the various modes of CO adsorption was somehow precluded by a strong contribution coming from the support, possibly due to its partial superficial reduction.

To sum up, the interaction of phosphorous with Rh showed several positive effects: (i) it formed a metallic surface capable to strongly adsorb CO; (ii) it improved the metal dispersion on the alumina support; (iii) it significantly inhibited the strong sulphur adsorption and lowered the resulting surface S coverage with special regards to those sites capable of strong CO adsorption.

According to TPR results, not all of the phosphorous interacted with Rh to form a new metallic phase in the Rh-P/LA catalyst; thus it can be argued that an even better S-tolerance might be achieved if one manages to force the formation of the Rh-P active phase.

3.2. CPO performance testing

After stabilization of the CPO performance of the Rh-P/LA honeycomb monolith under self-sustained conditions at $CH_4/O_2 = 2$ in air (T_{cat} = 730 °C, complete O_2 conversion), the impact of sulphur was studied by following the transient response of the catalytic reactor to a step addition of SO_2 to the feed. The typical temporal profiles of methane conversion, temperature inside the catalyst (T_{cat}) and selectivity to CO and H_2 are reported in Fig. 5a–d for the addition and subsequent removal of 20 ppm of SO_2. In line with recent results with Rh catalysts supported on various stabilized aluminas [10–13,15] the step addition of S to the feed to the Rh-P/LA honeycomb CPO reactor resulted in a rapid decrease in CH_4 conversion and selectivity to H_2, which was accompanied by a corresponding sharp increase in the catalyst temperature (ca. +160 °C), whereas the selectivity to CO was only marginally reduced. Such peculiar behaviour has been associated [12,13] to the inhibiting effect of sulphur on the kinetics of the endothermic methane steam reforming reaction (Eq. (1)), which significantly contributes to syngas formation over Rh catalyst [58,59] consuming part of the heat generated by the catalytic oxidation reactions. At the same time oxygen conversion from Rh-P/LA CPO reactor (not shown) remained complete, in good agreement with results of Bitsch-Larsen et al. [12] who

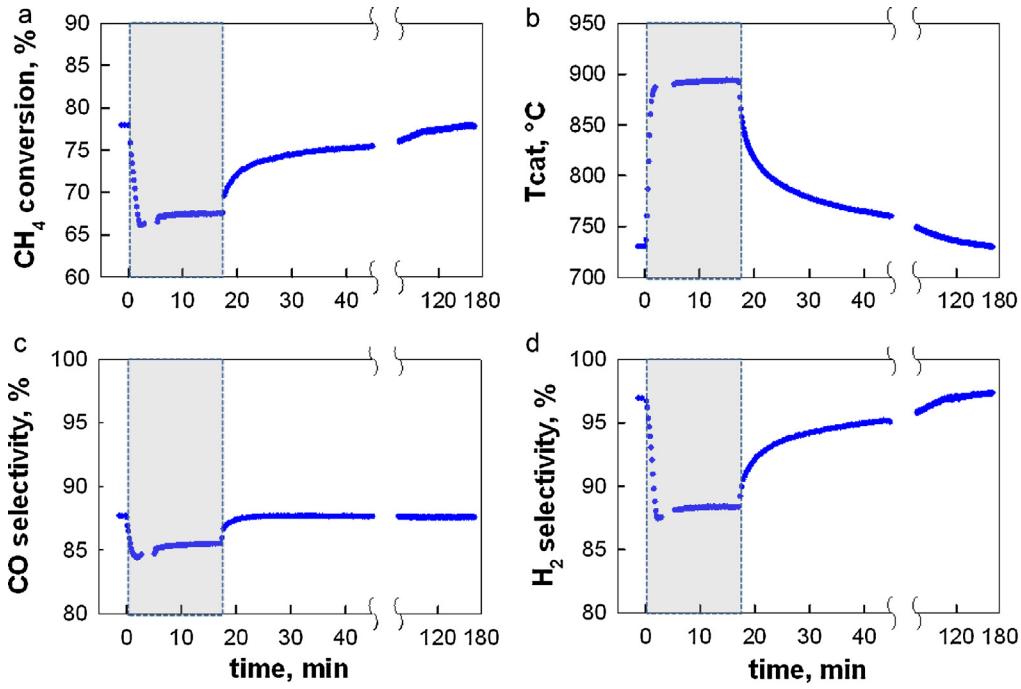

Fig. 5. Transient response to SO_2 addition (20 ppm) and removal during the CPO of methane on Rh-P/LA honeycomb: (a) methane conversion, (b) temperature in the middle of catalyst, selectivities to (c) CO and (d) H_2. Feed $CH_4/O_2 = 2$, air as oxidant.

reported that the rates of O_2 consumption on Rh (i.e. O_2 spatial profiles along the CPO reactor) were independent of the sulphur level, likely because the kinetics of the oxidation reactions remained much faster than the transport phenomena even in the presence of sulphur.

$$CH_4 + H_2O \leftrightarrow CO + 3H_2 \quad \Delta H_r^{25^\circ C} = +206\,kJ/mol \tag{1}$$

For each level of S in the feed (up to 58 ppm) the Rh-P/LA catalyst reached a novel steady state within ca. 10–15 min, without any visible sign of further loss/modification of its catalytic performance during time on stream in the presence of SO_2, at least on a time scale of a few additional hours (not shown). That suggests a dynamic equilibrium between S adsorbing on the surface of the active sites and S desorbing into the gas phase, which is governed by the catalyst temperature and sulphur concentration [13].

Upon removing the SO_2 from the reaction feed, the activity/selectivity of the Rh-P/LA catalyst was found to increase immediately although it required a relatively longer time in order to completely recover the initial levels, as opposed to the fast regeneration occurring on the undoped Rh/LA catalyst [13]. Therefore the interaction between Rh and P, which was shown to reduce the amount of S taken up by the metal, slowed down the desorption of a part of the surface S via reaction with gas phase H_2. A similar slow recovery effect was previously observed due to the presence of Ce in a Rh/CeO_2-γ-Al_2O_3 foam catalyst [12]. The complete reversibility of the S-poisoning effect under the studied reaction condition was also confirmed by the unchanged values of the temperatures measured at three different locations along the reactor before the addition and after the removal of sulphur, indicating the development of identical temperature (and reactivity) profiles inside the catalytic honeycomb.

Having ruled out any further decay of activity induced by progressive S-poisoning, steady state performance of Rh-P/LA and reference Rh/LA monolith [13] can be compared in Fig. 6a–c as a function of the S load in the feed. Under S free conditions both Rh based honeycombs displayed similar performance in terms of CH_4 conversion and yield to CO and H_2. This result is particularly significant in view of the lower loading of active washcoat on the Rh-P/LA honeycomb (0.11 g/cm^3) with respect to its Rh/LA counterpart (0.17 g/cm^3, [13]), which was completely compensated by the larger active surface area of the Rh-P/LA catalyst (Table 3). In fact it was demonstrated that during methane CPO over structured Rh-based catalysts, oxidation reactions are so fast to proceed under fully external mass transfer control [14,58,59]; on the other hand, the catalytic methane steam reforming is a much slower reaction that occurs under kinetic control on Rh, spreading all over the catalytic reactor [14]. The Water Gas Shift reaction (Eq. (2)) is generally equilibrated at the exit of Rh-based CPO reactors [3,57].

$$CO + H_2O \leftrightarrow CO_2 + H_2 \quad \Delta H_r^{25^\circ C} = -14\,kJ/mol \tag{2}$$

Our results suggest that the addition of phosphorous to Rh with the possible formation of a new metallic phase enhanced the intrinsic activity for methane steam reforming (per gram of catalyst), likely through the increased metal dispersion, while not significantly affecting the oxidation reaction path. This contrasts with recent results showing an evident poisoning effect caused by the addition of P to a 2.5 w/w% Rh/α-Al_2O_3 catalyst during the steam methane reforming at 700 °C, which eventually resulted in the formation of carbon filaments with large rhodium particles at the tip [17]. Those authors reported a much lower initial dispersion of Rh on α-Al_2O_3 (ca. 10%), which was further decreased down to 3.6% (with Rh particles of ca. 30 nm) after the addition of 1 atom of P for every 5 atoms of Rh. The striking discrepancy in the effect of P may thus originate from differences in the initial metal dispersion, as well as from the lack of a H_2 pre-reduction at high temperature [17] which is required for a favourable structural reconstruction.

Upon addition of sulphur the extent of deactivation for the P-doped Rh catalyst was always significantly lower than for its metallic counterpart, as indicated by a higher methane conversion and yield to syngas (and particularly to H_2, Fig. 6a–c), and a corresponding smaller jump of the catalyst temperature. As an example, at the maximum S level added to the feed (58 ppm), the Rh-P/LA catalyst converted ca. 66.6% of methane, with 55% yield to H_2 and 56.5% yield to CO, as opposed to 62.5%, 48.5% and 54.6% measured

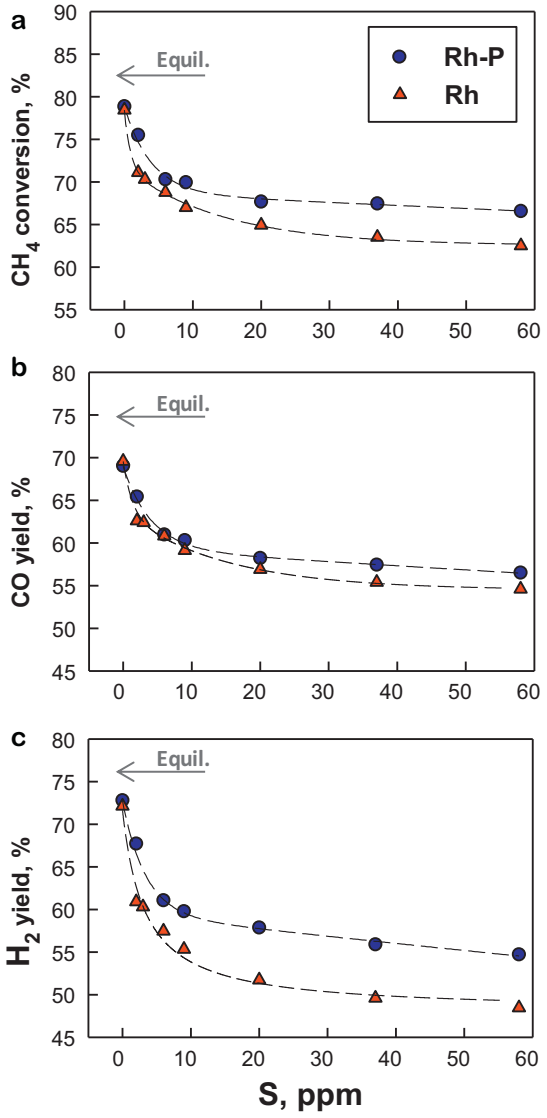

Fig. 6. Effect of SO_2 addition on CH_4 conversion (a), yield to CO (b) and to H_2 (c) from the CPO over Rh-P/LA and Rh/LA honeycomb catalyst. Feed $CH_4/O_2 = 2$, air as oxidant. Arrows indicate thermodynamic equilibrium values (P, h = constant).

respectively on the reference Rh/LA honeycomb; correspondingly, T_{cat} was observed to increase by 193 °C on Rh-P/LA, and by as much as 234 °C on Rh/LA catalyst, confirming the risk of overheating and permanent deactivation associated to autothermal operation in the presence of sulphur [14].

Fig. 7 shows that the temperature rise measured for each catalyst upon addition of any S level up to 58 ppm was proportional to the corresponding drop in methane conversion observed with respect to the S-free case. Starting from this observation, a simple heat balance on the gas phase was proposed [13] in order to calculate a lumped value for the heat of the reaction involving methane which was inhibited by S. From the slopes of the lines in Fig. 7 [13,15] this was estimated to be in the range +225–240 kJ/mol at 700 °C for both catalysts, which corresponds well to the heat of reaction for methane steam reforming (1) at that temperature. The inhibition of steam reforming is further corroborated by the change in the flows of products from Rh-P/LA catalyst induced by S-addition, exemplified in Table 4 for the case of 9 ppm SO_2 in the feed. In agreement with the results on Rh/LA [13] and Rh/CeO_2-γ-Al_2O_3 [12], the measured change in CO production corresponded to the drop in converted methane (i.e. unchanged S_{CO}), while the

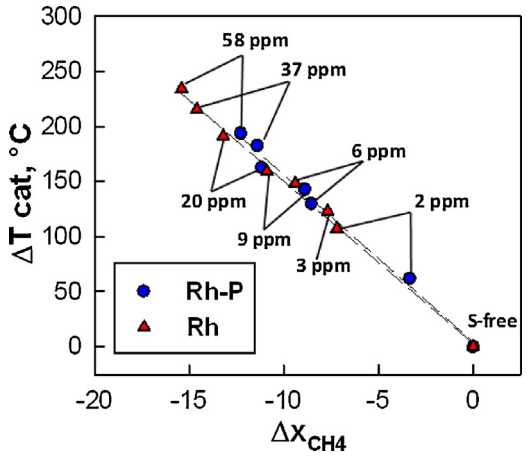

Fig. 7. Increase in catalyst temperature as a function of the variation of fuel conversion measured upon the addition of sulphur to the feed during the steady state CPO of methane over Rh-P/LA and Rh/LA honeycomb catalysts. Labels indicate sulphur content in the feed ($CH_4/O_2 = 2$ in air).

drop in the H_2 flow was almost three times larger, accordingly to the stoichiometry of reaction (1).

In order to better quantify the effect of sulphur [16,17] we calculated the experimental values of the proportionality constant for steam reforming (1) and water gas shift (2) reactions according to the definitions:

$$K_{exp,SR} = \frac{P_{H_2}^3 P_{CO}}{P_{H_2O} P_{CH_4}}; \quad K_{exp,WGS} = \frac{P_{H_2} P_{CO_2}}{P_{H_2O} P_{CO}}$$

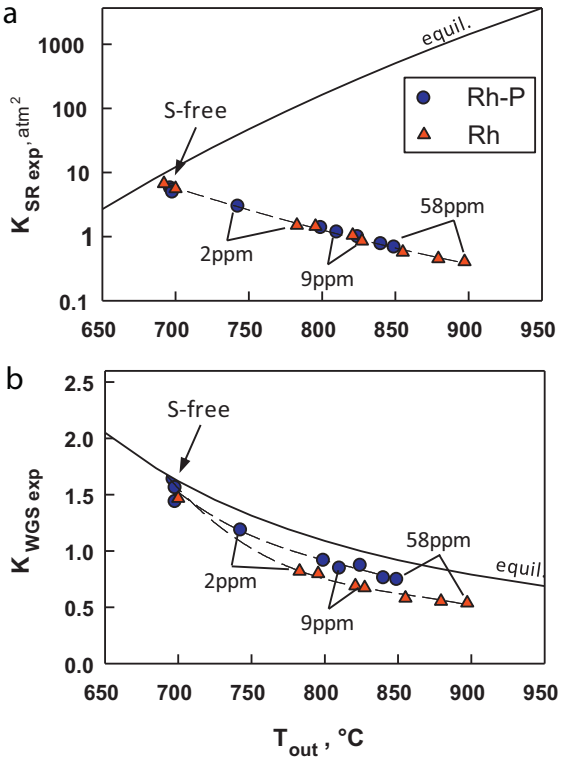

Fig. 8. Values of the proportionality constant for steam reforming (a) and water gas shift (b) reactions calculated at the exit temperature from Rh-P/LA and Rh/LA honeycomb catalysts during methane CPO under S-free operation and in the presence of SO_2 added to the feed (2–58 ppm). Continuous lines represent the equilibrium constants for each reaction at $P = 1.1$ atm.

Table 4
Changes in the steady state performance of methane CPO over Rh-P/LA honeycomb induced by the addition of 9 ppm SO_2. Feed $CH_4/O_2 = 2$, air as oxidant.

		SO_2		Differences[a]
$CH_4/O_2 = 2$		0 ppm	9 ppm	Δ (9 – 0)
X_{CH4}	(%)	78.9	70.0	−8.9
Y_{H2}	(%)	72.8	59.8	−26.0
Y_{CO}	(%)	69.0	60.3	−8.7
Y_{H2O}	(%)	6.1	10.2	+8.2
Y_{CO2}	(%)	9.9	9.7	−0.2

[a] Molar differences of each species produced from a feed of 100 CH_4.

Those values were compared (Fig. 8a,b) to the corresponding equilibrium constants K_{SR} and K_{WGS} calculated at the temperature measured at the exit of the catalytic honeycombs.

Under S-free conditions the WGS reaction was equilibrated with both catalysts; however the $K_{exp,SR}/K_{SR}$ ratio fell in the range 0.4–0.5, confirming that methane steam reforming was kinetically limited, which was expected also considering the heat losses from the CPO reactor, whose thermal efficiency was estimated at ca. 80–85% [60]. Sulphur addition progressively inhibited methane steam reforming without completely stopping it, as shown by the continuous decrease in the $K_{exp,SR}$ values, which followed the opposite trend of the equilibrium constant with temperature. Experimental data for the two catalysts collapsed in a single line because the temperature increase on both systems was indeed caused by the inhibition of the steam reforming. However P doping significantly enhanced the S tolerance of the Rh-P catalyst as shown by its higher $K_{exp,SR}$ at each S level (Fig. 8a).

The WGS reaction was also partially inhibited by sulphur on both Rh-based catalysts [16,17], but the detrimental effect was markedly lower than for steam reforming, and even smaller for Rh-P/LA as demonstrated by its closer approach to the equilibrium curve in Fig. 8b.

A rough and preliminary estimate of the impact of sulphur on the rate of methane steam reforming over the two catalysts was attempted through the inclusion of an "activity coefficient" in the kinetic expression [14], by assuming that sulphur only caused a reduction in the number of active sites (unchanged activation energy). The activity coefficient corresponds to the ratio of the pre-exponential factors in the SR kinetic constants with and without sulphur and it was estimated by the measured drop in methane conversion, taking into account the variation in the average temperature of the catalyst (second part of the reactor). The correction factor for the approach to equilibrium was neglected accordingly to the results of Fig. 8a. More details on simplifying assumptions and calculations are reported in the supplementary material.

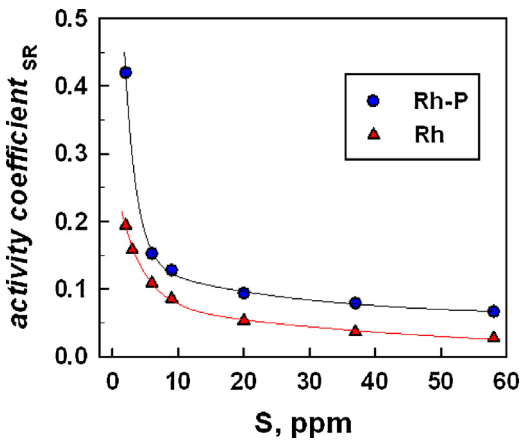

Fig. 9. Activity coefficient accounting for S poisoning of the steam reforming reaction over Rh-P/LA and Rh/LA honeycomb catalysts as a function of S level in the feed during methane CPO ($CH_4/O_2 = 2$ in air).

The activity coefficient values followed similar trends for the two catalysts (Fig. 9), decreasing markedly for the initial addition of few ppm of S to the feed, and then approaching a saturation value at the highest S levels. In particular for the Rh-P/LA catalyst the activity coefficient was estimated in the range from 0.4 to 0.1, being as much as 2 times higher than for the reference Rh/LA catalyst. Those results reflect the higher tolerance of P-promoted Rh towards strong sulphur chemisorption, which in turn translated into a higher residual active metal surface (Table 3). In fact activity coefficients suggest that the drop in the rate of methane steam reforming is mainly connected to the loss of those active sites capable of strongly chemisorb CO rather than on the total exposed metal sites [57].

4. Conclusions

A novel monolith catalyst with Rh supported on γ-alumina and doped with phosphorous was prepared by temperature-programmed reduction of oxidic precursors in flowing H_2, and it was tested for the first time in the CPO of methane at short contact time and high temperature in the presence of sulphur. The interaction of phosphorous with Rh showed several positive effects: (i) it formed a metallic surface capable to strongly adsorb CO; (ii) it improved the metal dispersion on the alumina support; (iii) it significantly inhibited the strong sulphur adsorption and lowered the resulting surface S coverage, with special regards to those sites capable of strong CO adsorption. Reaction of phosphorous with the alumina also enhanced the stability of the support, probably through the formation of surface $AlPO_4$, but it partially prevented a complete reaction of P with Rh. Direct comparison of CPO performance data with the reference undoped Rh catalysts showed a significant enhancement of the specific steam reforming reaction rate, which can be correlated to the higher metal dispersion, and markedly contrasts with previous reports on the poisoning effect of P on $Rh/\alpha\text{-}Al_2O_3$. Above all, the P doped Rh catalyst was significantly more S-tolerant then the reference undoped system, guaranteeing a higher methane conversion and H_2 selectivity at any S level in the feed up to 58 ppm, while reducing the risk of excessive catalyst overheating due to the S-inhibition of the endothermic steam reforming reaction path. The higher residual steam reforming activity of the Rh-P catalyst during the CPO of methane in the presence of sulphur appears to be correlated to the larger exposed active metal surface capable to strongly bond CO (as gem-dicarbonyl species) at room temperature.

Acknowledgement

Financial support from "MiSE-CNR Accordo di Programma per l'Attività di Ricerca di Sistema" under project: "Biocombustibili" is acknowledged.

Appendix A. Supplementary data

Supplementary data associated with this article can be found, in the online version, at http://dx.doi.org/10.1016/j.apcatb.2013.02.039.

References

[1] B. Enger, R. Lødeng, A. Holmen, Applied Catalysis A 346 (2008) 1–27.
[2] G.J. Panuccio, B.J. Dreyer, L.D. Schmidt, AIChE Journal 53 (2007) 187–195.
[3] B.C. Michael, A. Donazzi, L.D. Schmidt, Journal of Catalysis 265 (2009) 117–129.
[4] J.L. Colby, P.J. Dauenhauer, L.D. Schmidt, Green Chemistry 10 (2008) 773–783.
[5] P.J. Dauenhauer, B.J. Dreyer, N.J. Degenstein, L.D. Schmidt, Angewandte Chemie International Edition 46 (2007) 5864–5867.
[6] H.S. Gandhi, G.W. Graham, R.W. McCabe, Journal of Catalysis 216 (2003) 433–442.
[7] M. Machida, K. Murakami, S. Hinokuma, K. Uemura, K. Ikeue, M. Matsuda, M. Chai, Y. Nakahara, T. Sato, Chemistry of Materials 21 (2009) 1796–1798.
[8] C. Hulteberg, International Journal of Hydrogen Energy 37 (2012) 3978–3992.
[9] G.B. Fisher, K.M. Rahmoeller, C.L. DiMaggio, K. Wadu-Mesthrige, J.G. Weissman, E.C. Tan, L. Chen, J.E. Kirwan, North American Catalyst Society 20th North American Meeting, Huston TX June 17–22, 2007.
[10] S. Cimino, L. Lisi, Industrial and Engineering Chemistry Research 51 (2012) 7459–7466.
[11] J.K. Hong, L. Zhang, M. Thompson, W. Wei, K. Liu, Industrial and Engineering Chemistry Research 50 (2011) 4373–4380.
[12] A. Bitsch-Larsen, N. Degenstein, L. Schmidt, Applied Catalysis B 78 (2008) 364–370.
[13] S. Cimino, R. Torbati, L. Lisi, G. Russo, Applied Catalysis A 360 (2009) 43–49.
[14] A. Beretta, G. Groppi, M. Lualdi, I. Tavazzi, P. Forzatti, Industrial and Engineering Chemistry Research 48 (2009) 3825–3836.
[15] S. Cimino, L. Lisi, G. Russo, R. Torbati, Catalysis Today 154 (2010) 283–292.
[16] S. Cimino, L. Lisi, G. Russo, International Journal of Hydrogen Energy 37 (2012) 10680–10689.
[17] R. Chakrabarti, J.L. Colby, L.D. Schmidt, Applied Catalysis B 107 (2011) 88–94.
[18] C.H. Bartholomew, Applied Catalysis A 212 (2001) 17–60.
[19] R. Prins, M.E. Bussell, Catalysis Letters 142 (2012) 1413–1436.
[20] S.T. Oyama, T. Gott, H. Zhao, Y. Lee, Catalysis Today 143 (2009) 94–107.
[21] P. Clark, S.T. Oyama, Journal of Catalysis 218 (2003) 78–87.
[22] F. Sun, W. Wu, Z. Wu, J. Guo, Z. Wei, Y. Yang, Z. Jiang, F. Tian, C. Li, Journal of Catalysis 228 (2004) 298–310.
[23] A.W. Burns, K.A. Layman, D.H. Bale, M.E. Bussell, Applied Catalysis A 343 (2008) 6876.
[24] T. Montesinos-Castellanos, A. Zepeda, B. Pawelec, J.L.G. Fierro, J.A. de los Reyes, Chemistry of Materials 19 (2007) 5627–5636.
[25] S.J. Sawhill, K.A. Layman, D.R. Van Wyk, M.H. Engelhard, C. Wang, M.E. Bussell, Journal of Catalysis 231 (2005) 300–313.
[26] Z. Wu, F. Sun, W. Wu, Z. Feng, C. Liang, Z. Wei, C. Li, Journal of Catalysis 222 (2004) 41–52.
[27] J. Hayes, R. Bowker, A. Gaudette, M. Smith, C. Moak, C. Nam, T. Pratum, M. Bussell, Journal of Catalysis 276 (2010) 249–258.
[28] Y. Kanda, C. Temma, K. Nakata, T. Kobayashi, M. Sugioka, Y. Uemichi, Applied Catalysis A 386 (2010) 171–178.
[29] C.M. Sweeney, K.L. Stamm, S.L. Brock, Journal of Alloys and Compounds 448 (2008) 122–127.
[30] E.L. Muetterties, J.C. Sauer, Journal of the American Chemical Society 96 (1974) 3410–3415.
[31] D. Wang, O. Dewaele, A.M. Groote, G.F. Froment, Journal of Catalysis 159 (1996) 418.
[32] R. Torbati, S. Cimino, L. Lisi, G. Russo, Catalysis Letters 127 (2009) 260–269.
[33] C. Xie, Y. Chen, M. Engelhard, C. Song, ACS Catalysis 2 (2012) 1127–1137.
[34] K. Ikeue, K. Murakami, S. Hinokuma, K. Uemura, D. Zhang, M. Machida, Bulletin of the Chemical Society of Japan 83 (2010) 291–297.
[35] S. Cimino, G. Landi, L. Lisi, G. Russo, Catalysis Today 117 (2006) 454–461.
[36] V. Perrichon, L. Retailleau, P. Bazin, M. Daturi, J.C. Lavalley, Applied Catalysis A 260 (2004) 1–8.
[37] A. Maroto-Valiente, I. Rodriguez-Ramos, A. Guerrero-Ruiz, Catalysis Today 93–95 (2004) 567–574.
[38] S. Trautmann, M. Baerns, Journal of Catalysis 150 (1994) 335–344.
[39] J. Raskó, J. Bontovics, Catalysis Letters 58 (1999) 27–32.
[40] E. Finocchio, G. Busca, P. Forzatti, G. Groppi, A. Beretta, Langmuir 23 (2007) 10419–10428.
[41] L. Erdey, S. Gál, G. Liptay, Talanta 11 (1964) 913–940.
[42] C.-P. Hwang, C.-T. Yeh, Q. Zhu, Catalysis Today 51 (1999), 93-10.
[43] A. Boumaza, L. Favaro, J. Lédion, G. Sattonnay, J.B. Brubach, P. Berthet, A.M. Huntz, P. Royc, R. Tetot, Journal of Solid State Chemistry 182 (2009) 1171–1176.
[44] F. Solymosi, M. Pasztor, Journal of Physical Chemistry 89 (1985) 4789–4793.
[45] D.K. Paul, C.D. Marten, J.T. Yates Jr., Langmuir 15 (1999) 4508–4512.
[46] P. Basu, D. Panayotov, J.T. Yates, Journal of the American Chemical Society 110 (1988) 2074–2081.
[47] K.A. Layman, M.E. Bussell, Journal of Physical Chemistry B 108 (2004) 10930–10941.
[48] K.I. Hadjiivanov, G.N. Vayssilov, Advanced Catalysis 47 (2002) 307–511.
[49] D.A. Bulushev, G.F. Froment, Journal of Molecular Catalysis A: Chemical 139 (1999) 63–72.
[50] S.D. Jackson, B.J. Brandreth, D. Winstanley, Journal of the Chemical Society, Faraday Transactions 1 (83) (1987) 1835–1842.
[51] M.A. Newton, A.J. Dent, S. Diaz-Moreno, S.G. Fiddy, B. Jyoti, J. Evans, Chemical Communications 0 (2003) 1906–1907.
[52] B. McAllister, P. Hu, Journal of Chemical Physics 122 (2005) (Article number 84709).
[53] J. Oudar, Catalysis Reviews-science and Engineering 22 (1980) 171–195.
[54] Y. Konishi, M. Ichikawa, W. Sachtler, Journal of Physical Chemistry 91 (1987) 6286–6291.
[55] N.S. Nasri, J.M. Jones, V.A. Dupont, A. Williams, Energy and Fuels 12 (1998) 1130–1134.
[56] S.S. Chuang, S.-I. Pien, C. Sze, Journal of Catalysis 126 (1990) 187–191.
[57] J. Wei, E. Iglesia, Journal of Catalysis 225 (2004) 116–127.
[58] R. Horn, K.A. Williams, N.J. Degenstein, A. Bitsch-Larsen, D. Dalle Nogare, S.A. Tupy, L.D. Schmidt, Journal of Catalysis 249 (2007) 380–393.
[59] R. Horn, K.A. Williams, N.J. Degenstein, L.D. Schmidt, Journal of Catalysis 242 (2006) 92–102.
[60] S. Cimino, L. Lisi, G. Mancino, M. Musiani, L. Vázquez-Gómez, E. Verlato, International Journal of Hydrogen Energy 37 (2012) 17040–17051.